A fuzzy logic controlled Anti-lock Braking System (ABS) for improved braking performance and directional stability

Article *in* International Journal of Vehicle Design · January 2008

DOI: 10.1504/IJVD.2008.022581

Y. Samim Unlusoy
Middle East Technical University

A fuzzy logic controlled Anti-lock Braking System (ABS) for improved braking performance and directional stability

Yigit Yazicioglu* and Y. Samim Unlusoy

Mechanical Engineering Department,
Middle East Technical University,
06531 Ankara, Turkey
E-mail: yigit@metu.edu.tr
E-mail: unlusoy@metu.edu.tr
*Corresponding author

Abstract: A simple and effective fuzzy logic controller is designed for an Anti-Lock Braking System (ABS) to improve the braking performance and directional stability of an automobile during braking, and steering-braking maneuvers on uniform and nonuniform (μ-split) friction surfaces. The system consists of two controllers working in tandem. The first controller works on the longitudinal slip, and the second controller is responsible for the side-slip motion control of the vehicle. The fuzzy logic controller is implemented on a four-wheel nonlinear vehicle model with nonlinear tyre behaviour. Simulations are carried out and comparisons are made using the vehicle model with and without the fuzzy logic controlled ABS to assess controller performance.

Keywords: ABS; anti-lock braking system; fuzzy control; nonlinear vehicle model; nonlinear tyre model; vehicle dynamic simulation.

Reference to this paper should be made as follows: Yazicioglu, Y. and Unlusoy, Y.S. (xxxx) 'A fuzzy logic controlled Anti-lock Braking System (ABS) for improved braking performance and directional stability', *Int. J. Vehicle Design*, Vol. x, No. x, pp.xxx–xxx.

Biographical notes: Yigit Yazicioglu obtained his PhD in Mechanical Engineering from the University of Illinois at Chicago, USA. Currently, he is an Assistant Professor at the Department of Mechanical Engineering, Middle East Technical University, Ankara, Turkey. He teaches courses and performs research activities in the areas of dynamics and control, vehicle dynamics, robotics, vibration and acoustics.

Y. Samim Unlusoy obtained his PhD in Mechanical Engineering from the University of Birmingham, UK. Currently, he is a Professor at the Middle East Technical University, Ankara, Turkey, where he teaches courses and leads project and research teams on automotive engineering. His research interests include vehicle dynamics and automatic control systems.

1 Introductıon

The ability to provide for the reduction of its speed quickly and in a stable manner is one of the vital functions of a motor vehicle. A large proportion of situations threatening the safety of a moving vehicle occur while the driver tries to decelerate or stop the vehicle in a situation involving one or more of the following:

- braking on slippery surfaces
- braking and cornering (or steering to avoid an obstacle)
- braking on a surface with asymmetric friction coefficients (μ-split surfaces).

In most of the accidents, an obstacle appears in front of the vehicle and the driver has to take action after recognising the danger. This action depends on many parameters such as the distance between the vehicle and the obstacle, the state of the other lanes – being occupied or not – the condition of the road surface, etc. A vehicle without an Anti-lock Braking System (ABS) is safe only when there is sufficient clearance before the obstacle, the road is straight, and the coefficient of friction is the same for the left and right side of the vehicle. If any of these conditions do not apply, single or multiple vehicle crashes may occur. Even with an ABS with only longitudinal motion control capability, single vehicle crashes are not a far risk.

The idea of Anti-Lock Braking goes as far back as 1930s with the first examples appearing in aerospace applications in around 1950s. ABS emerged in early 1970s on passenger cars (Douglas and Schafer, 1971) to assist automobile drivers, enhancing stability and increasing braking capability and quickly became standard equipment on most vehicles. There is extensive literature on ABS studies and an effort will be made to mention those related to this study. Examples of cited work involving general control strategies are by Kraft and Leffler (1990), Yi et al. (2003) and Sugai et al. (1999). Research on ABS technology continued in the form of applying various control strategies on the same principle. Two examples are Mazumdar and Lim (1995) and Wang and Zhou (2000), regarding the use of neural networks with slip control braking algorithms. In the field of robust control, the study carried out by Yu (1997) is a fine example. Numerous efforts appear in the domain of sliding-mode control applied to ABS controller design. Some of the commonly cited work is due to Chin et al. (1992), Choi and Cho (1999), Drakunov et al. (1995), Kawabe et al. (1997) and Will et al. (1998). Also a sample of four references are due to Chen and Wu (2004), Layne et al. (1993), Mirzaei et al. (2005) and Will and Zak (2000) about fuzzy algorithms utilised, one of which is the application on a motorcycle. With the advance of brake-by-wire technologies and possible widespread near future use of hybrid vehicles, it will be possible to use different actuation hardware in ABS. Studies concerning these issues are many, but the work of Anwar (2004), Emereole and Good (2005) and Kees et al. (2001) provide a good summary. In all the cases, generation of accurate braking commands depend on good knowledge of vehicle states and friction prediction and cited work in this area is given in the works of Daiss and Kiencke (1995), Kobayashi et al. (1995) and Samadi et al. (2001).

Most of the studies encountered in literature have concentrated on the slip control aspect of the braking phenomena, considering straight line braking with uniform friction surfaces. The stability aspect involving braking during cornering or braking on μ-split surfaces have not received equal emphasis, and studies of Ayalew et al. (2004), Hebden et al. (2004) and Taheri and Law (1991) are the exceptions where this aspect is addressed in particular.

Recently, ABS has been included in the integrated active safety system, known generally as Electronic Stability Program (ESP), together with Traction Control System (TCS) and Active Yaw Control (AYC). The fact that ESP seems to control the yaw stability of the vehicle through AYC, however, is not to be interpreted as reducing ABS to longitudinal slip control only. It must be remembered that ESP is reserved, at least for the time being, for higher segment of vehicles or as an expensive option, and is not as common as ABS. Thus, for those vehicles equipped with ABS only, improving ABS to control stability in addition to longitudinal slip would be significant. Further, it may also contribute to the development of ESP systems.

A fuzzy logic controller, which consists of two controllers working in parallel, is proposed in this study. The first controller works on the longitudinal slip, and the second controller is responsible for the side-slip motion control of the vehicle. It is implemented on a four-wheel nonlinear vehicle model with nonlinear tyre behaviour. Simulations with and without the fuzzy logic controlled ABS are carried out to assess the controller performance and the results illustrate the benefits of the proposed controller.

2 Mathematical model

The mathematical model for the vehicle used in this study consists of three parts; the tyre model, the vehicle body model, and the fuzzy logic controller. These will be discussed briefly in the following.

2.1 Nonlinear tyre model

In a vehicle dynamical model, tyre forces result in the most significant changes in the states of the vehicle. Thus, the tyre model must be accurate and reliable, covering a wide range of operating conditions. Tyre model presented by Allen et al. (1987) is selected for use in this study. Allen model is an accurate, nonlinear model taking numerous parameters of a tyre into consideration for the calculation of lateral and longitudinal forces. This tyre model is used because it responds realistically over the full maneuvering range under large longitudinal slip ratios and lateral slip angles. Longitudinal and lateral tyre forces, F_x and F_y, can be calculated for any longitudinal slip ratio, S, and lateral slip angle, α. in the following form, normalised in $\mu \cdot F_z$, the maximum tractive force,

$$\frac{F_x}{\mu F_z} = \frac{-f(\sigma)k_c' S}{\sqrt{k_s^2 \tan^2 \alpha + k_c'^2 S^2}} \tag{1}$$

$$\frac{F_y}{\mu F_z} = \frac{f(\sigma)k_s \tan\alpha}{\sqrt{k_s^2 \tan^2 \alpha + k_c'^2 S^2}} \tag{2}$$

where the empirical relations for 'slide' friction coefficient, μ, composite slip function, σ, force saturation function, $f(\sigma)$, lateral stiffness coefficient, k_s, and modified longitudinal stiffness coefficient, k_c, are provided in Allen et al. (1987). These relations require some parameters to be obtained from experimental analysis and from the tyres physical properties. This makes the tyre model perform very close to the real tyre behaviour.

With this sophisticated tyre model, various plots can be generated depicting the complete behaviour of a tyre. Two important plots are presented here in the Figure 1 for nominal friction coefficient of 0.85, normal tyre load of 3000 N and vehicle speed of 72 km/h, using data for a wide section low profile radial tyre.

Figure 1 Normalised braking force vs. longitudinal slip ratio (top) normalised cornering force vs. lateral slip angle (bottom)

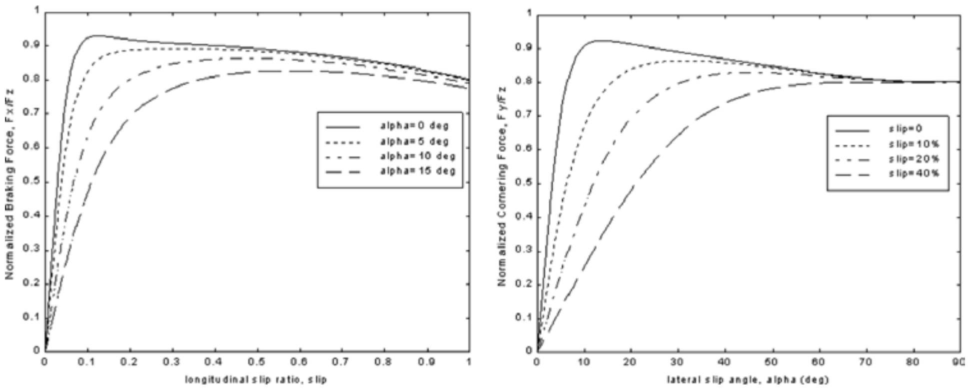

2.2 Nonlinear vehicle model

For automobiles, vehicle models vary from simplest two-wheeled linear bicycle model to four-wheeled nonlinear, multi-body models. In this study, the behaviour of the vehicle when braked during cornering and μ-split surfaces will be of interest and the longitudinal, lateral, and yaw motions are all significant. Thus, a four-wheeled vehicle model is selected, Figure 2. It can simulate the behaviour of the vehicle in the longitudinal, lateral, and yaw directions resulting from the tyre forces developed by the four individual tyres. The lateral and longitudinal weight transfers are made closer to reality by the addition of quasistatic and uncoupled roll and pitch dynamics of the vehicle caused by the lateral and longitudinal acceleration during cornering and braking.

The motion of the vehicle body is described by six variables; three of which are the longitudinal velocity, lateral velocity, and yaw velocity. The remaining three are the position variables determining the location of the vehicle on the plane of the road. Further, each wheel has a rotational degree of freedom uncoupled from the vehicle dynamics. A detailed formulation of the vehicle model is presented by Yazıcıoglu (1999).

The states of the system are changed by the external traction and cornering forces. The independent external inputs are the steering angle of the front wheels and/or the individual wheel braking moments. The changes in longitudinal and lateral slip values trigger lateral and/or longitudinal tyre forces to develop and differing tyre forces manipulate the states. The block diagram of this closed loop dynamical system showing the flow of simulation is shown in Figure 3.

Figure 2 Vehicle model with (a) tyre force interactions and (b) roll and pitch degrees of freedom

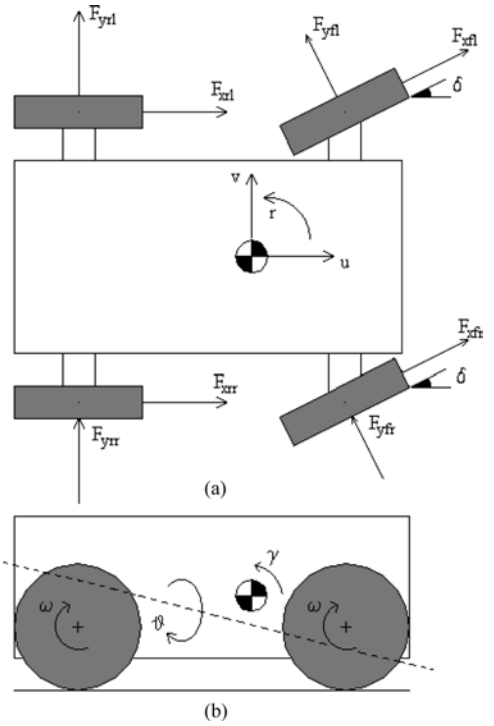

Figure 3 Block diagram of the simulated vehicle dynamic model and closed loop control system

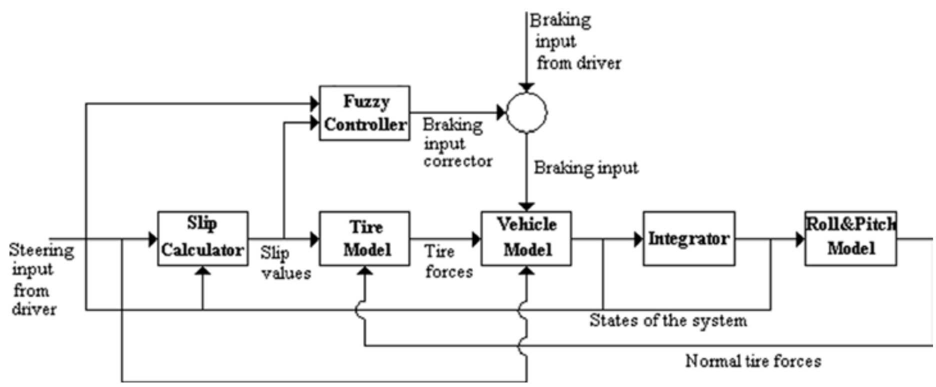

The equations of motion of the vehicle may be written in the general form below, where u, v, and r denote the longitudinal, lateral, and yaw velocities; δ_{ij} are the steering angle inputs to the front wheels; and M_{bij} are the braking moment inputs to individual wheels.

$$\dot{u} = \frac{1}{M}(F_{xfl}\cos\delta_{fl} + F_{xfr}\cos\delta_{fr} + F_{xrl} + F_{xrr} - F_{yfl}\sin\delta_{fl} - F_{yfr}\sin\delta_{fr}) + vr \tag{3}$$

$$\dot{v} = \frac{1}{M}(F_{xfl}\sin\delta_{fl} + F_{xfr}\sin\delta_{fr} + F_{yfl}\sin\delta_{fl} + F_{yfr}\sin\delta_{fr} + F_{yrl} + F_{yrr}) - ur \tag{4}$$

$$\dot{r} = \frac{1}{I}[a(F_{xfl}\sin\delta_{fl} + F_{yfl}\cos\delta_{fl} + F_{xfr}\sin\delta_{fr} + F_{yfr}\cos\delta_{fr}) + b(-F_{yrl} - F_{yrr})]$$
$$+\frac{1}{I}\left[\frac{t_f}{2}(-F_{xfl}\cos\delta_{fl} + F_{yfl}\sin\delta_{fl} + F_{xfr}\cos\delta_{fr} - F_{yfr}\sin\delta_{fr}) + \frac{t_r}{2}(-F_{xrl} + F_{xrr})\right]. \quad (5)$$

Here, M and I are mass and moment of inertia, respectively. Also, a, b, t_f, and t_r are front axle distance to center of mass, rear axle distance to center of mass, front track width, and rear track width, respectively. In addition, for each wheel with radius R and moment of inertia, I_w, the uncoupled dynamic equation is,

$$\dot{\omega}_{ij} = \frac{1}{I_w}(-F_{xij}R - M_{bij}), \quad ij = fl, fr, rl, \text{and } r. \quad (6)$$

Finally, equations related to the positioning of the vehicle in an earth fixed reference frame are given where x and y are the coordinates of the mass center in fixed frame and ψ is the yaw angle.

$$\dot{x} = u\cos\psi - v\sin\psi \quad (7)$$

$$\dot{y} = u\sin\psi + v\cos\psi \quad (8)$$

$$\dot{\psi} = r. \quad (9)$$

The form of the nonlinear equations of motion makes the use of a marching numerical method possible. Since the nonlinearities of the functions are smooth, with the use of small time steps, accurate and fast calculations can be achieved.

2.3 Fuzzy logic controller

The fuzzy controller proposed in this work consists of two parts, longitudinal slip controller and side-slip controller, Figure 4. Objective of the slip controller is executing the fuzzy rule set to keep the longitudinal slip values of the tyres within a desired range specified by the construction of the respective membership functions. By careful analysis of Figure 1, it can be seen that the maximum value of braking force is usually obtained at longitudinal slip values ranging from 0.025 to 0.125 for friction coefficient values between 0.2 and 1.0. This controller works on the longitudinal slip input according to the estimated coefficient of friction. The effect of tyre-road friction coefficient is reflected in the membership functions, especially by considering the tyre behaviour on different friction conditions and setting the target longitudinal slip values in the membership functions accordingly. It gives out a correction value to the braking moment input that the driver applies by the brake pedal.

However, for an ABS control of longitudinal slip towards maximum braking performance is not the only problem. Cornering force, which is the main factor for cornering ability for the vehicle, depends on the longitudinal slip ratio besides the lateral slip angle. A small amount of increase in longitudinal slip results in a very steep decrease in lateral force generating ability. Thus, the cost of a small improvement in braking distance may be a large reduction in the directional control and also lateral stability of a vehicle. Usually, the ability of changing direction provides a better advantage in emergency situations, than ability to stop in a shorter distance. This can be seen in Figure 1 on the graph showing the variation of cornering forces at different longitudinal slip ratios. Obviously, proper use of both is the best and this is possible through the use of a correctly tuned ABS, which does not merely control the longitudinal slip for stopping distance but also cares for increasing the cornering ability.

Figure 4 Schematic of the controller

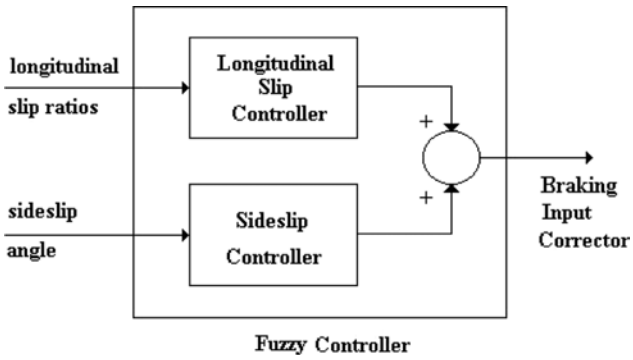

The second controller is responsible for the side-slip motion control of the vehicle. The side-slip angle of a vehicle may change under the effect of different traction forces on the left and right wheel pairs. The driver may not be able to control this motion due to the large force difference between the two sides of the vehicle. By using the relevant fuzzy rule set and operating on the sideslip angle, β, which is defined as,

$$\beta = \tan^{-1}\left(\frac{v}{u}\right), \tag{10}$$

the second controller gives out another yaw generating moment correction on top of the correcting moment by the first controller to minimize sideslip angle as can be seen from the related membership functions. The combination of the two single input-single output sub controllers, results in a double input-single output overall controller. The output of the controller is converted to the rate of change of the braking moment. The current brake force is modified with this value at each time step of the controller. The dynamical behaviour of the braking system is neglected. It is assumed that the output command of the controller is physically realisable as a zeroth order response.

Throughout the study Mamdani fuzzy inference method is implemented in MATLAB software. The fuzzy controller uses very simple inside arithmetics. The '*and*' operator and implication are realised by '*min*' function, the '*or*' operator and aggregation are by 'max' function, the defuzzification is performed by the '*centroid method*'.

The input and output variables of the longitudinal slip and side-slip controllers have five membership functions (triangular and trapezoidal) each, as shown as an example in Figure 5. Friction coefficient range, from 0 to 1.2, is divided into three zones namely, dry, wet, and ice for the friction coefficient ranges of 0 to 0.3, 0.3 to 0.7, and 0.7–1.2, respectively. For each zone, a different set of membership functions drive the slip controller. The sideslip angle controller uses a single membership function definition for all friction zones.

Figure 5 Membership functions for the longitudinal slip (dry road set is given as example) (top) and side-slip controller (bottom)

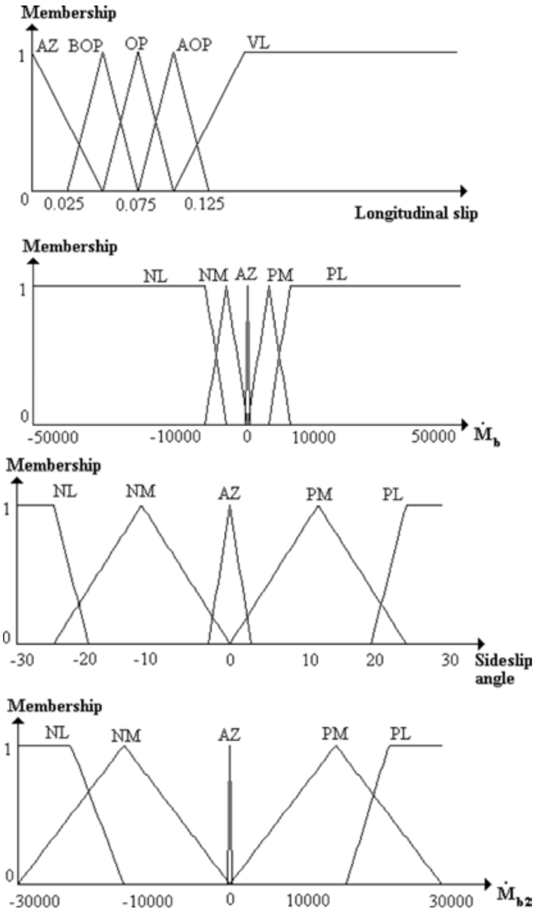

The rules operating the slip controller are as follows:

- if longitudinal slip (S) is Very Large (VL), then rate of change of braking moment $(\dot{M}_b)$ is Negative Large (NL)
- if longitudinal slip (S) is Approximately Zero (AZ), then rate of change of braking moment $(\dot{M}_b)$ is Positive Large (PL)
- if longitudinal slip (S) is Optimum (OP), then rate of change of braking moment $(\dot{M}_b)$ is AZ
- if longitudinal slip (S) is Below Optimum (BOP), then rate of change of braking moment $(\dot{M}_b)$ is Positive Medium (PM)
- if longitudinal slip (S) is Above Optimum (AOP), then rate of change of braking moment $(\dot{M}_b)$ is Negative Medium (NM).

The rules operating the side-slip controller are as follows:

- if sideslip angle (β) is NL, then rate of change of braking moment for side-slip control $(\dot{M}_{b2})$ is NL
- if sideslip angle (β) is NM, then rate of change of braking moment for side-slip control $(\dot{M}_{b2})$ is NM
- if sideslip angle (β) is AZ, then rate of change of braking moment for side-slip control $(\dot{M}_{b2})$ is AZ
- if sideslip angle (β) is PM, then rate of change of braking moment for side-slip control $(\dot{M}_{b2})$ is PM
- if sideslip angle (β) is PL, then rate of change of braking moment for side-slip control $(\dot{M}_{b2})$ is PL.

The controller first checks if the brake is applied. If it is not, zero output is produced. Then for each wheel the lock condition is checked. Lock condition takes place if longitudinal slip value exceeds a predetermined value, i.e., 0.1. If a wheel locks first, the correcting moment for the slip controller is evaluated by using the longitudinal slip ratio at that wheel. After that, vehicle sideslip angle is checked for its sign and value and the correcting moment from the side-slip controller is calculated by using the sideslip angle. If that wheel is not locked, then both of the correcting moments are zero. The corrections are imposed on the driver's braking input as seen below.

$$M_{b_{n+1}} = M_{b_n} + \dot{M}_{b1_n}\Delta t + \dot{M}_{b2_n}\Delta t. \tag{11}$$

2.4 Estimation of unmeasured states

Ordinarily in a normal vehicle, the only measured state is the peripheral wheel velocity of the vehicle. For vehicles with slip control systems, this information may be used together with the peripheral acceleration of wheels to have an idea of the amount of longitudinal slip. But this is only an estimate and this procedure can give poor results. This can be better understood when the longitudinal slip for any wheel is presented for a four wheeled vehicle.

$$S_{ij} = \frac{v_{wlij} - \omega_{ij} R}{v_{wlij}}, \quad ij = fl, fr, rl, rr. \tag{12}$$

In the above equation *vwl* is the vehicle velocity in the plane of the wheel and as an example given below for the front-left wheel.

$$v_{wlfl} = \sqrt{\left(u - r\frac{t_f}{2}\right)^2 + (v + ar)^2} \cos\alpha_{fl}. \tag{13}$$

Obviously this requires the knowledge of vehicle longitudinal, lateral and yaw velocities, as well as the lateral slip angle for that specific wheel,

$$\alpha_{fl} = \delta_{fl} - \tan^{-1}\left(\frac{v + ar}{u - r\dfrac{t_f}{2}}\right) \tag{14}$$

also given as a sample for front-left side, which also requires velocity knowledge for accurate control. Similarly, the estimation of sideslip angle, β (equation (10)), also depends on these velocities. Ergo, a possible solution is to install a pair of orthogonal accelerometers and a rate gyro in the yaw plane of the vehicle, to measure the longitudinal, lateral, accelerations and yaw velocity. If the measured longitudinal and lateral accelerations, and yaw velocities at time step n are P_n, Q_n, and R_n, respectively, then the values of the longitudinal, lateral, velocities at time step $n + 1$ may be calculated numerically.

$$u_{n+1} = u_n + (P_n + v_n R_n)\Delta t \tag{15}$$

$$v_{n+1} = v_n + (Q_n - u_n R_n)\Delta t. \tag{16}$$

Since the rotational velocities of the wheels are directly measured, the rest of the variables can be calculated by the controller circuit. The approximate friction coefficient may also be found by simply normalising the longitudinal acceleration by the gravitational acceleration. This estimated value is used by the controller to decide on which membership function set should be used for longitudinal slip control.

$$\mu_{\text{nom}} = \frac{P}{g}. \tag{17}$$

Sensing the pitch angle by means of another sensor such as an inclinometer will render this estimation more accurate to discard the effects of pitch changes due to longitudinal acceleration and road inclination angles.

In real applications, noise and errors in the measured data may cause problems, but by appropriate filtering and signal conditioning techniques accurate results may be obtained with current state of the art. These aspects of the study is beyond the scope of this work. It is breifly mentioned in this section to demonstatrate the possible challenges in the methodology.

3 Simulation results

This work is performed for a typical mid-size vehicle with given dimensional and inertial data in Table 1. The vehicle is expected to display understeer behaviour.

Table 1 Vehicle data

M (kg)	I (kg·m^2)	a (m)	b (m)	R (m)	I_w (kg·m^2)	t_f (m)	t_r (m)
1300	1620	1.0	1.45	0.33	2.03	1.45	1.45

First, to display the handling performance of the simulated vehicle some results are provided in Figure 6 for a step steering command of 2° on the front wheels without braking. The simulated vehicle behaves as expected, attaining approximately 20 m lateral deflection in 3 s of simulation. To assess the performance of the fuzzy logic controller, three different braking modes are considered:

- straight-line braking on uniform friction surface
- braking and steering on uniform friction surface
- braking on a μ-split surface.

Figure 6 Step steering response without braking vs. time, sideslip angle (top-left), yaw velocity (top-right), lateral acceleration (bottom-left), lateral slip angles (bottom-right)

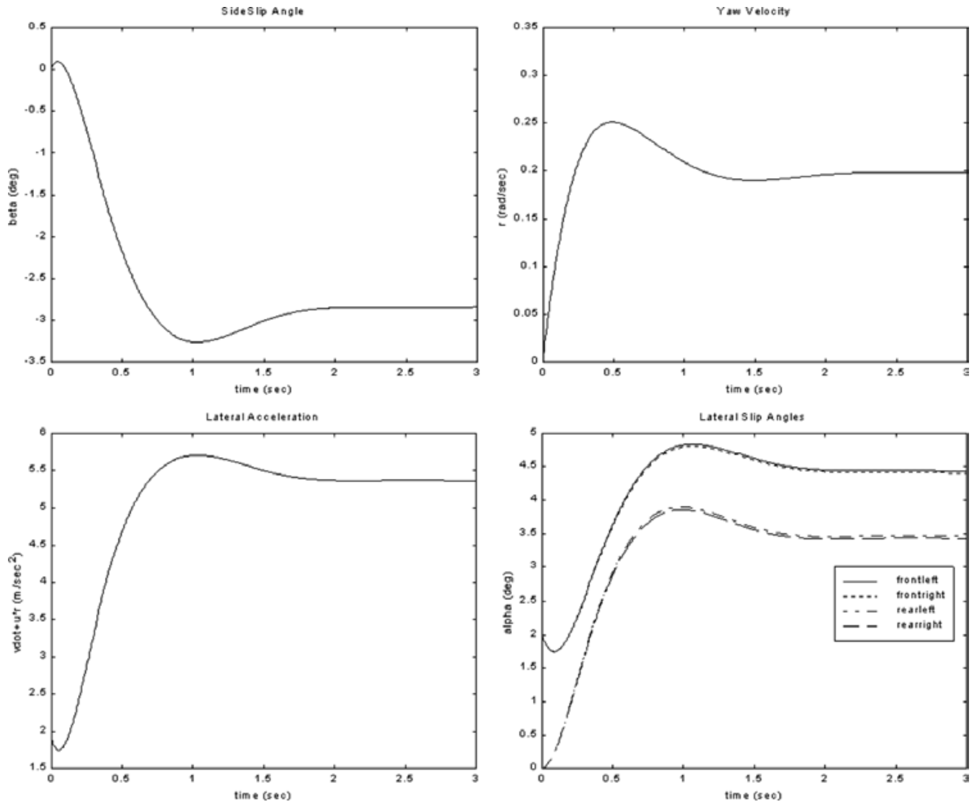

Braking simulations are carried out, first for an automobile with conventional (non-ABS) brakes, and then for the same vehicle equipped with the fuzzy logic controlled ABS. Three kinds of road surfaces, i.e., dry, wet, and ice with nominal coefficient of friction values 0.85, 0.5, and 0.15, respectively, are considered. For the dry and wet surface conditions, the initial velocity is taken as 100 km/h. For icy road surface, the initial speed is reduced to 50 km/h. A total braking torque of 3000 Nm is applied as a step input, which can quite closely mimic the conditions during an emergency situation. The initial braking torque distribution is taken as 70 % for the front and 30% for the rear wheels. The reference values for the longitudinal slip ratios are pre-specified as 0.075 that can be seen on the longitudinal slip membership function in Figure 5. When steering is involved, the steering angle of the front wheels is taken to be 2°, which is also applied as a step input.

Sample results for straightline braking favors the ABS equipped vehicle. Figure 7 shows the longitudinal accelerations side by side showing clearly that ABS exploits the nonlinear tyre's traction behaviour, which explains the shorter stopping distance. In addition, the controller's corrective effort and its effect on longitudinal slip is shown.

Figure 7 Straight-line panic braking, longitudinal acceleration w/o ABS (top-left), with ABS (top-right), longitudinal slip ratio w/o ABS (middle-left), with ABS (middle-right), corrective torque rates (bottom-left), peripheral wheel speeds (bottom-right) (see online version for colours)

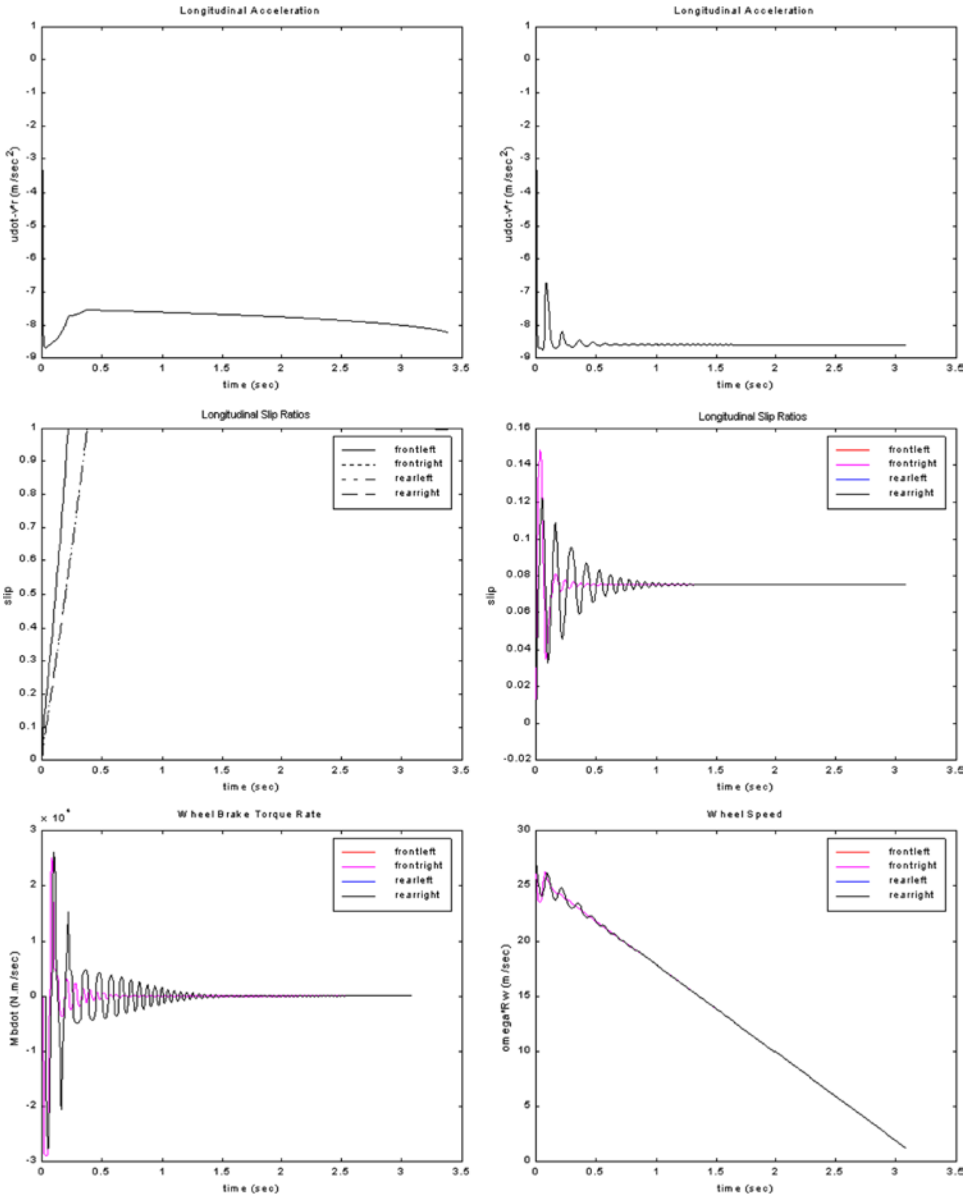

The breaking and steering simulation is important because it shows the results of the ability of the vehicle to gain lateral deflection during maximum deceleration. Just clearing a road obstacle may not be safe because other encounters may occur after the first obstacle is cleared. Both of the steering and braking actions must take place in a stable manner for safest results. Without an ABS this manoeuvre yields strong deceleration with no lateral deflection capability if the braking and steering commands are simultaneously applied. A driver may even lose control and spin out, as it is successfully observed in the simulations here with various magnitudes of braking and steering performed in the name of controlled panic braking in an obstacle avoiding manoeuvre. Such a case is presented in Figure 8 where a third of the braking torque is applied and the vehicle is steered to clear the obstacle but the yaw velocity is unstable and the vehicle spins out. On the contrary, Figure 9 shows some selected results for hard braking and steering manoeuvre with ABS showing effective results. It is seen that sideslip angle is stable with good lateral acceleration made possible.

Figure 8 Yaw velocity for slight braking and steering

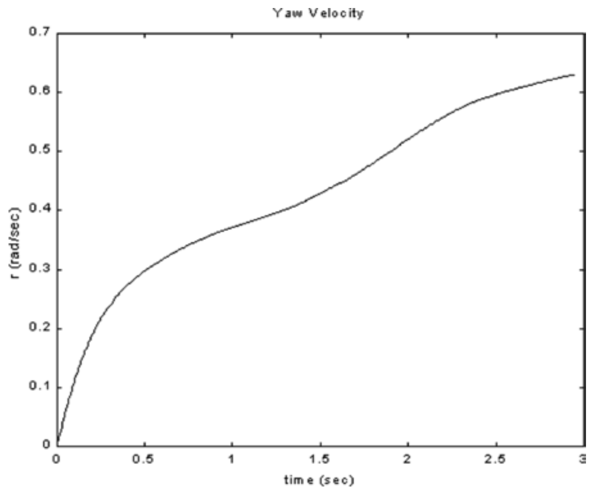

Finally, braking on μ-split surface is simulated and comparisons are made between ABS equipped and unequipped vehicle. The μ-split condition is simulated as a friction coefficient of 1.2 on the left side and 0.7 on the right side. This can be the case where the left side is on dry surface and the right side on wet asphalt or gravel. Simulations show that hard braking on such a surface gives no chance to the driver as the yaw velocity shoots up and side slip angle becomes unmanagable (~30°) in a short while (~1 s). Figure 10 shows selected traces of the simulated response on μ-split. One can see the stabilised sideslip angle with the help of ABS due to heavy braking moment correction on the left-side of the vehicle from the side-slip controller.

The results obtained from the tests on the vehicle without the ABS and with the fuzzy ABS are shortly discussed below and summarised in Table 2. Results for wet and icy road conditions are not given due to limited space. For those cases membership functions are constructed accordingly but a common sideslip controller is used. Anyhow, the results are similar in terms of cornering ability, lateral deflection and vehicle dynamic stability, the only difference being the longer braking duration and larger stopping distances than the dry case.

Figure 9 Panic braking with steering, lateral acceleration without ABS (top-left), with ABS (top-right), longitudinal slip and side-slip controller efforts (middle-left and right), wheel brake torques (bottom-left), sideslip angle (bottom -right) (see online version for colours)

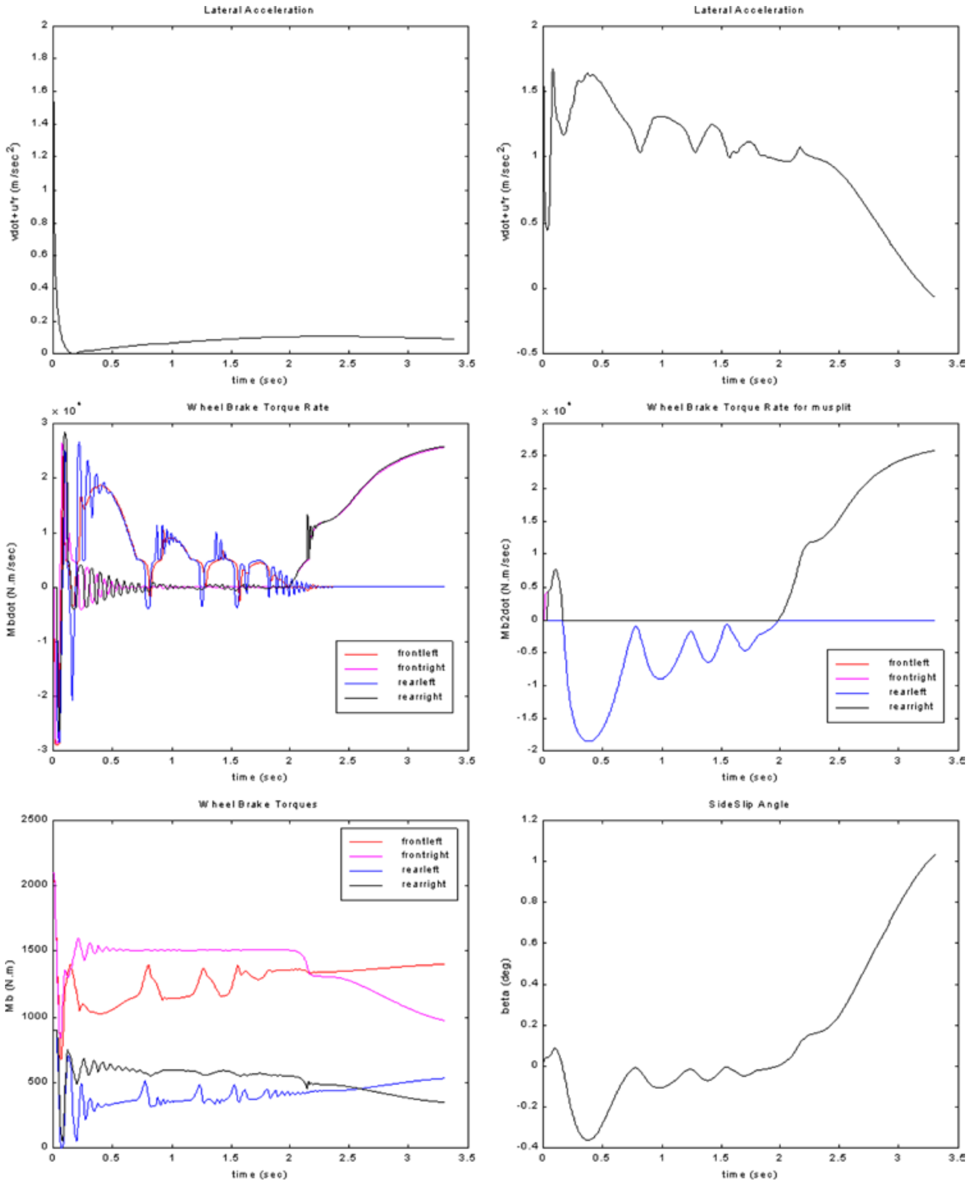

Figure 10 Panic braking on µ-split, yaw velocity w/o ABS (top-left), side-slip angle with ABS (top-right), longitudinal slip and side slip angle controller efforts (middle-left and right), wheel brake torques (bottom-left), longitudinal acceleration (bottom-right) (see online version for colours)

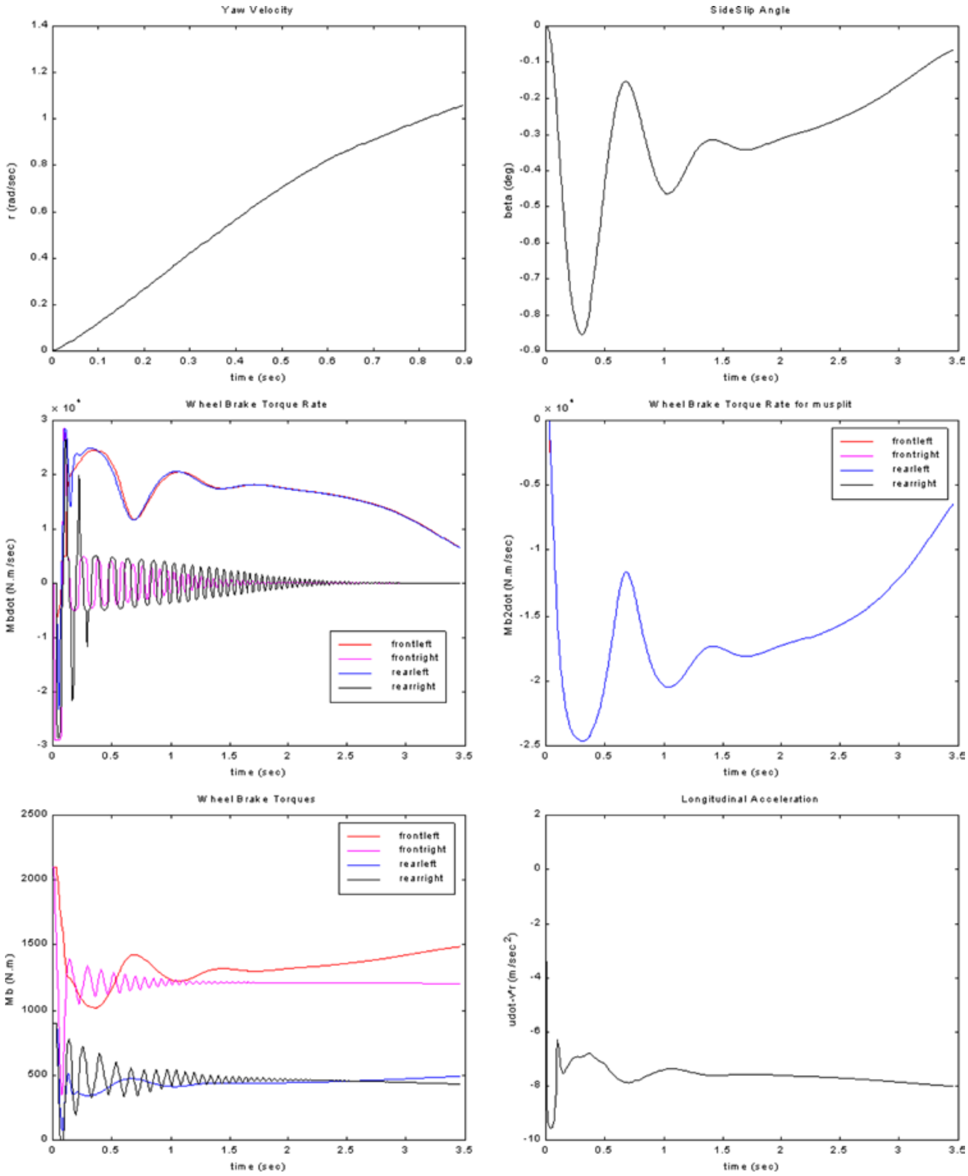

Table 2 Simulation results

	Without ABS (*dry surface*)		*With FUZZY ABS* (*dry surface*)	
SMB	Vehicle stopped with all wheels locked immediately		Vehicle stopped with oscillating manipulated input until 1 s	
	x (m)	49.8	x (m)	45.3
B&S	Vehicle stopped with all wheels locked. Could not be steered		Vehicle stopped while it was possible to steer with a small sideslip angle	
	x (m)	49.8	x (m)	47.7
	y (m)	~0	y (m)	3.4
	ψ (°)	0.7	ψ (°)	14.0
	$\lvert\beta\rvert$ (°)	~0	$\lvert\beta\rvert$ (°)	<1
μSP	Vehicle spun out before 1 s has passed when u = 62.5 km/h		Vehicle stopped without spinning out with a small deflection. Can be recovered	
	x (m)	21.5	x (m)	51.1
	y (m)	~0	y (m)	1.3
	ψ (°)	30.2	ψ (°)	4.5
	$\lvert\beta\rvert$ (°)	–30	$\lvert\beta\rvert$ (°)	<1

4 Conclusions

Simulated results show that during straight motion braking, there is a 10% difference in the braking distances favouring the vehicle with the fuzzy logic controlled ABS. Further, the lateral stability of the vehicle with fuzzy ABS is better, because none of the wheels of the vehicle with ABS are locked or kept at high longitudinal slip ratios, making it possible for the tyres to generate forces in the lateral direction. For the case of braking and steering at the same time (B&S), the results indicate a definite improvement with the use of the fuzzy ABS. The vehicle with the fuzzy ABS stops safely in a shorter distance and also it is able to displace from its initial line of travel at an amount, which is equal to more than a lane's width. This can be increased if desired by tuning the fuzzy controller to shoot for a smaller reference longitudinal slip at the cost of increased braking distance. Due to the present sideslip controller its sideslip angle, β, is kept very small. When the vehicle has to slow down on a μ-split road, the vehicle without ABS is in a dangerous situation. This vehicle immediately loses its stability giving almost no chances to the driver to counter-steer to remain on the course. This may sometimes be a more dangerous condition than actually hitting the obstacle. When it comes to the vehicle with the sideslip controlling fuzzy ABS, as soon as the driver steps on the brakes, the controller takes control of the situation and helps the vehicle stop with a smooth deceleration and a controllable and small deflection from its initial course.

Due to its flexible design this vehicle model and the fuzzy controller can be also used to study traction control and ESP with minor modifications on the present code.

References

Allen, R.W., Rosenthal, T.J. and Szostak, H.T. (1987) *Steady State and Transient Analysis of Ground Vehicle Handling*, SAE Paper 870495.

Anwar, S. (2004) 'An anti-lock braking control system for a hybrid electromagnetic/electro hydraulic brake-by-wire system', *Proceedings of the American Control Conference*, Vol. 3, pp.2699–2704.

Ayalew, B., Muthiah, S., Yu, N. and Kulakowski, B.T. (2004) 'A study of combined braking and cornering performance of a transit bus using validated computer simulation', *American Society of Mechanical Engineers, Design Engineering Division (Publication) DE*, Vol. 117, pp.883–892.

Chen, C. and Wu, J. (2004) 'Development of fuzzy controlled ABS systems for motorcycles', *International Journal of Vehicle Design*, Vol. 34, No. 1, pp.84–100.

Chin, Y., Lin, W.C., Sidlosky, D.M., Rule, D S. and Sparschu, M.S. (1992) 'Sliding-mode ABS wheel-slip control', *Proceedings of the American Control Conference*, Vol. 1, pp.1–5.

Choi, S. and Cho, D. (1999) 'Control of wheel slip ratio using sliding mode controller with pulse width modulation', *Vehicle System Dynamics*, Vol. 32, No. 4, pp.267–284.

Daiss, A. and Kiencke, U. (1995) 'Estimation of vehicle speed fuzzy estimation in comparison with Kalman-filtering', *Proceedings of the IEEE Conference on Control Applications*, pp.281–284.

Douglas, J. and Schafer, T. (1971) *The Chrysler 'Sure-Brake:' The First Production Four-Wheel Anti-Skid System*, SAE Paper 710248.

Drakunov, S., Ozguner, U., Dix, P. and Ashrafi, B. (1995) 'ABS control using optimum search via sliding modes', *IEEE Transactions on Control Systems Technology*, Vol. 3, No. 1, pp.79–85.

Emereole, O.C. and Good, M.C. (2005) 'Comparison of the braking performance of electromechanical and hydraulic ABS systems', *American Society of Mechanical Engineers, Dynamic Systems and Control Division (Publication) DSC*, Vol. 74 (1 PART A), pp.319–328.

Hebden, R.G., Edwards, C. and Spurgeon, S.K. (2004) 'Automotive steering control in a split-μ manoeuvre using an observer-based sliding mode controller', *Vehicle System Dynamics*, Vol. 41, No. 3, pp.181–202.

Kawabe, T., Nakazawa, M., Notsu, I. and Watanabe, Y. (1997) 'A sliding mode controller for wheel slip ratio control system', *Vehicle System Dynamics*, Vol. 27, Nos. 5–6, pp.393–408.

Kees, M., Burnham, K.J., Lockett, F.P., Tabor, J.H. and Williams, R.A. (2001) 'Hydraulic actuated brake and electromechanically actuated brake systems', *IEE Conference Publication*, Vol. 483, pp.43–47.

Kobayashi, K., Cheok, K.C. and Watanabe, K. (1995) 'Estimation of absolute vehicle speed using fuzzy logic rule-based Kalman filter', *Proceedings of the American Control Conference*, Vol. 5, pp.3086–3090.

Kraft, H.J. and Leffler, H. (1990) 'Integrated brake and stability control system of the new BMW 850i', *SAE Transactions*, Vol. 99, No. 6, pp.291–299.

Layne, J.R., Passino, K.M. and Yurkovich, S. (1993) 'Fuzzy learning control for antiskid braking systems', *IEEE Transactions on Control Systems Technology*, Vol. 1, No. 2, pp.122–129.

Mazumdar, S.K. and Lim, C.C. (1995) 'Investigation of the use of neural networks for anti-skid brake system design', *Proceedings of the World Congress on Intelligent Control and Automation (WCICA)*, Vol. 2, pp.1018–1021.

Mirzaei, A., Moallem, M. and Mirzaeian, B. (2005) 'Designing a genetic-fuzzy anti-lock brake system controller', *Proceedings of the IEEE International Symposium on Intelligent Control*, Vol. 2, pp.1246–1250.

Samadi, B., Kazemi, R., Nikravesh, K.Y. and Kabganian, M. (2001) 'Real-time estimation of vehicle state and tire-road friction forces', *Proceedings of the American Control Conference*, Vol. 5, pp.3318–3323.

Sugai, M., Yamaguchi, H., Miyashita, M., Umeno, T. and Asano, K. (1999) 'New control technique for maximizing braking force on antilock braking system', *Vehicle System Dynamics*, Vol. 32, No. 4, pp.299–312.

Taheri, S. and Law, E.H. (1991) 'Slip control braking of an automobile during combined braking and steering maneuvers', *American Society of Mechanical Engineers, Design Engineering Division Publication DE*, Vol. 40, pp.209–227.

Wang, N. and Zhou, C. (2000) 'A neuron controller with self-tuning gain for anti-lock braking systems', *Proceedings of the IEEE International Symposium on Intelligent Control*, pp.505–510.

Will, A.B., Hui, S. and Zak, S.H. (1998) 'Sliding mode wheel slip controller for an antilock braking system', *International Journal of Vehicle Design*, Vol. 19, No. 4, pp.523–539.

Will, A.B. and Zak, S.H. (2000) 'Antilock brake system modelling and fuzzy control', *International Journal of Vehicle Design*, Vol. 24, No. 1, pp.1–18.

Yazicioglu, Y. (1999) *Development of a Fuzzy Controlled ABS to Improve Braking Performance and Stability of Automobiles*, Unpublished M.S. Thesis, Mechanical Engineering Department, Middle East Technical University, Ankara, Turkey.

Yi, J., Alvarez, L., Claeys, X. and Horowitz, R. (2003) 'Emergency braking control with an observer-based dynamic tire/road friction model and wheel angular velocity measurement', *Vehicle System Dynamics*, Vol. 39, No. 2, pp.81–97.

Yu, J.S. (1997) 'Robust adaptive wheel-slip controller for antilock brake system', *Proceedings of the IEEE Conference on Decision and Control*, Vol. 3, pp.2545–2546.